

## INVESTIGATION OF TIP CLEARANCE EFFECT ON LOSSES USING LARGE EDDY SIMULATION

Erkan Kocaoglu\*, Abdurrahman G. Yavuz† and Ayse G. Gungor‡

Faculty of Aeronautics and Astronautics, Istanbul Technical University, Istanbul, Turkey

### ABSTRACT

*This study presents a numerical investigation of tip clearance size effect on the tip leakage flow in a linear turbine cascade. Analysis are performed using an open source flow solver, OpenFOAM. Two gap sizes, %0.5 and %1.5 of span are studied by using large eddy simulation (LES) technique. Results are validated with mean pressure coefficient values and energy density spectrum. The leakage flow and its effect on the main stream increases significantly as the gap size increases. The main influence of the gap size is to increase the emerging jet flow, which interacts with the main separated region and hence triggers early transition. The strength of the secondary flow structures and hence pressure losses increase in the high clearance case.*

### INTRODUCTION

The aerodynamic performance of modern turbomachines are limited by some types of loss mechanisms. The most crucial of these loss mechanisms is the tip leakage loss. In turbines, there must be a clearance between the blade and the tip end-wall because of thermal expansion, rubbing and the manufacturing limitations. The secondary flow structures and losses occur in the turbine because of this clearance. Previous studies have shown that about 30% of the aerodynamic losses in a turbine is due to the tip leakage [Denton, 1993; Andichamy et al., 2018].

The tip leakage flow takes place when the flow passes from pressure side to suction side from clearance as shown in figure 1. When the tip leakage occurs, pressure loss is formed on the blade and this affects the main flow. The tip leakage flow encounters an adverse pressure gradient in the gap and separates from the end-wall forming a vortex structure at downstream of the gap [Lompart et al., 2004]. Due to the tip leakage vortex, a loss of loading occurs towards the tip of the blade [Trehan and Roy, 2012]. The flow separates due to the sharp corner at the entrance of clearance and creates a separation bubble. No separation bubble occurs when the clearance height is low or the blade is thinner [Andichamy et al., 2018]. The flow between the separation bubble and the casing wall accelerates, and then turn into a jet flow in the gap. In addition, the tip leakage flow is accelerated in the tip gap because of the significant pressure gradient [Lompart et al., 2004]. Previous studies show that negative effects of the tip leakage increase with increasing clearance size. Hence reducing the tip gap size would reduce losses and enhance efficiency [Volino, 2017]. Furthermore, engine fuel consumption, service life and

---

\*Aeronautical Engineer, Turkish Aerospace, Ankara Email: kocaoglu16@itu.edu.tr

†MSc Student in Aeronautical and Astronautical Engineering, Email: yavuzabd@itu.edu.tr

‡Assoc. Prof. in Faculty of Aeronautics and Astronautics, Email: ayse.gungor@itu.edu.tr

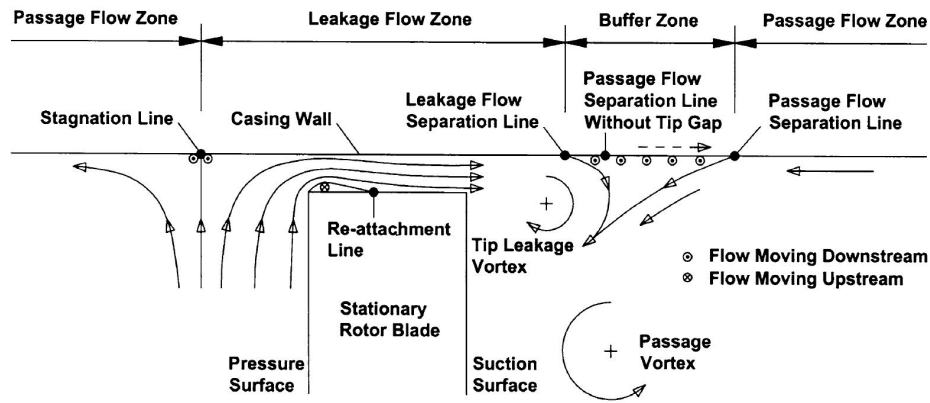


Figure 1: Tip leakage mechanism [Lee and Kim, 2010].

the exhaust gas temperature margin can be improved as increased turbine efficiency [Lei and Yanpei, 2014].

Studies are carried out to understand and obstruct tip leakage structures that affect aerodynamics performance of turbines by researchers for a long time. Morphis and Bindon [Morphis and Bindon, 1994] studied the tip clearance loss and divided it into two main categories in a linear turbine. The first one is the entropy caused by the leakage flow through the gap and the second one is the leakage flow leaving the gap and mixing with the main stream. They also showed that tip clearance phenomena depends on the blade profile. Tallman and Lakshminarayana [Tallman and Lakshminarayana, 2001] studied effect of tip clearance height and outer casing relative motion. They had two different tip clearance heights, %1 and %2.5 percent of the span length. Results show that mass flow rate through tip clearance gap is %3.9 more for %2.5 clearance than that of %1, with respect to the passage mass flow rate. Tip leakage vortices are significantly stronger as the clearance size is increased. For the relative casing wall study, the size of the tip leakage vortex for moving wall is third of the fixed wall. Total pressure losses due to tip leakage dominated other secondary losses for the fixed wall case. However, such losses were in the same range for the relative motion case. That means that real operating conditions, the presence of the moving wall, reduces tip leakage effect. Andichamy et al. [Andichamy et al., 2018] studied the detailed of tip leakage interrupters. The clockwise induced vortex is created with tip leakage interrupters placed on the suction side. As a result, the strength of the counterclockwise rotating tip leakage vortex is reduced.

The present study aims to investigate the tip leakage flow over a low-pressure turbine (LPT) blade to contribute further understanding of the tip leakage flow mechanism. Specifically, the effect of tip gap size on the tip leakage flow will be analyzed in detail. For this purpose, two gap sizes, %0.5 and %1.5 of the span are investigated by using large eddy simulation (LES) technique. Effects of gap size on secondary structures and losses are investigated for both cases.

## NUMERICAL DETAILS

Numerical simulations have been performed by using an open-source computational fluid dynamics solver OpenFOAM. PISO algorithm is used for the solution of the incompressible LES equations along with the widely-used k- $\epsilon$  subgrid model. The unshrouded T106 LPT blade, whose specifications are presented in Table 1 is used for the analysis. The computational domain with boundary conditions and a detailed view of the grid near the tip clearance are illustrated in figure 2. The cyclic boundary condition is imposed along the pitch-wise direction to include the effects of neighbouring blades on the flow field. No-slip boundary condition is imposed for the blade and the tip end wall. Half span is used for all simulations with a symmetry boundary condition to reduce computational expenses. Inlet boundary layer condition influences three-dimensionality of the flow around a LPT blade [Cay, 2018].

**Table 1:** T106 blade specification.

Chord	198	[mm]	Suction surface length	264.7	[mm]
Axial Chord	170	[mm]	Pressure surface length	230.0	[mm]
Blade Stagger	30.7	[°]	Inlet flow angle	37.7	[°]
Pitch	158	[mm]	Design exit flow angle	63.2	[°]
Span	200	[mm]			

The simulations are performed with a turbulent boundary layer inlet condition, which is imposed as mean velocity profile with a shape factor of 1.5.

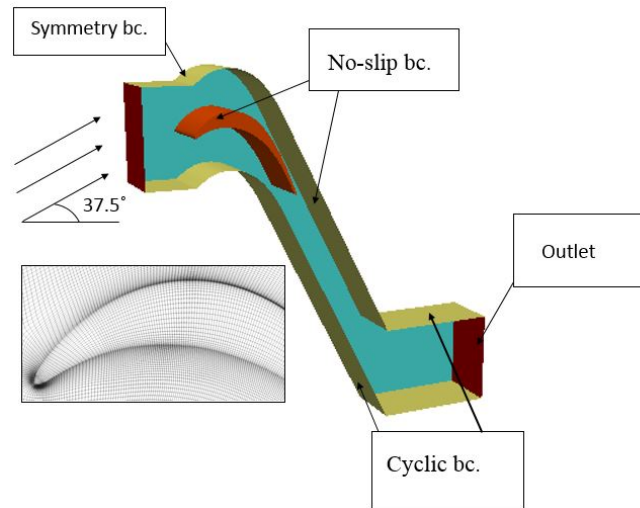


**Figure 2:** Computational domain with boundary conditions; inlet and outlet (red), periodic surfaces (yellow) and the tip end wall (blue) and grid detail near tip clearance.

The solution strategy consists of two phases as high clearance case that has 18.5 million hexahedral elements and low clearance case that has 15 million hexahedral elements. The numerical details and  $y^+$  values along the surface of the blade and also the casing wall are given in Table 2. Furthermore, the energy density spectrum is obtained to examine the quality of the grids for LES results. A probe located in the wake region beyond the trailing edge and very close to the tip gap is used to collect temporal information of velocity fluctuations. As shown in Figure 3, LES results follow the Kolmogorov's  $-5/3rd$  law at least a decade for both cases. This is considered reasonable for LES studies.

**Table 2:** Numerical details.

	Gap Size	Mesh	Surface	$y^+$
Case 1	%1.5	18.5M	Blade	2.4
			Casing wall	1
Case 2	%0.5	15M	Blade	3
			Casing wall	1

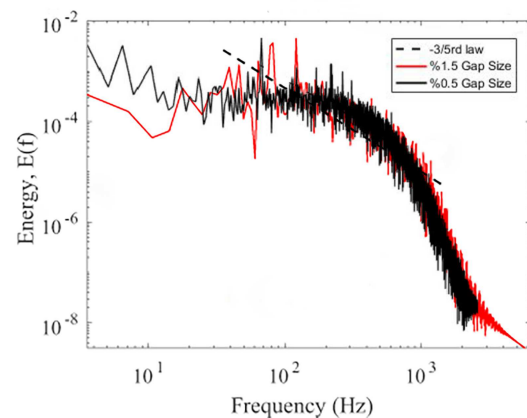


**Figure 3:** The energy density spectrum..

The analysis are performed at Reynolds number of  $8 \times 10^4$ , matching the available experimental data for T106 turbine blade. For both simulations, turbulent statistics are accumulated for 7 flow through times (FTT) after an initial transient of 5 FTT.

## RESULTS AND DISCUSSION

The instantaneous flow structures are visualized using the second invariant of the velocity gradient tensor and shown in figure 4 for 0.5% and 1.5% clearance sizes. The incoming flow deviates from the leading edge owing to the presence of blade, and generates a horseshoe vortex. This vortex can be also qualified as a blockage structure. This horseshoe vortex separates into two different legs which are named as pressure and suction side legs of the horseshoe vortex. Flow leaks from the sharp corner of the pressure side of the blade to the suction side, and forms the tip leakage vortex. The tip leakage effect increases as the tip gap size increases. The strength and organization of the vortical structures on the suction surface for the large clearance case significantly differs from the small clearance one.

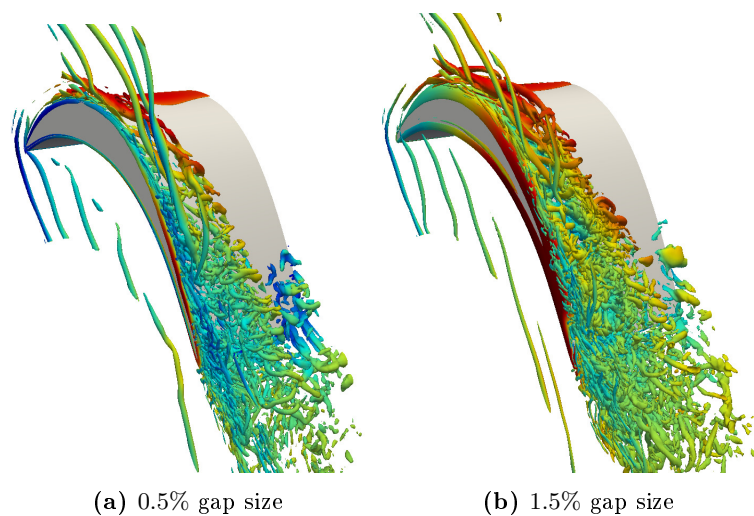


**Figure 4:** Instantaneous vortical structures colored with axial velocity.

Figure 5 depicts the instantaneous visualizations of the streamlines that pass from the clearance for two gap sizes. The tip leakage effect extends all the way up to the half-span, indicating the significant alternation of the primary flow (separated region due to APG) on the suction surface due to enhanced leakage for high clearance. It is also clear that the affected flow transitions earlier in the case of high clearance as compared to the low clearance case.

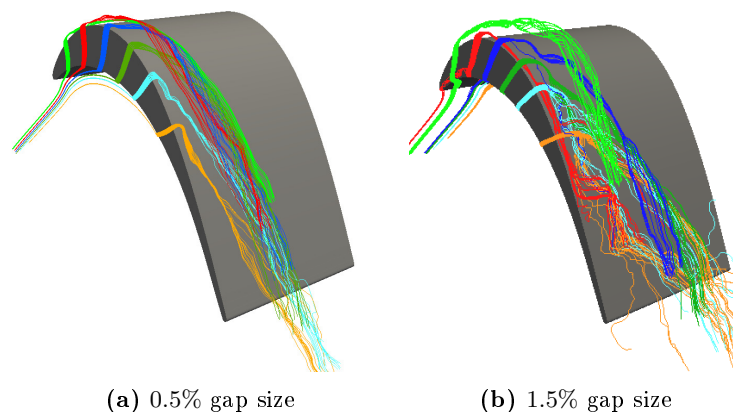


**Figure 5:** Instantaneous visualizations of streamlines that pass from clearance.

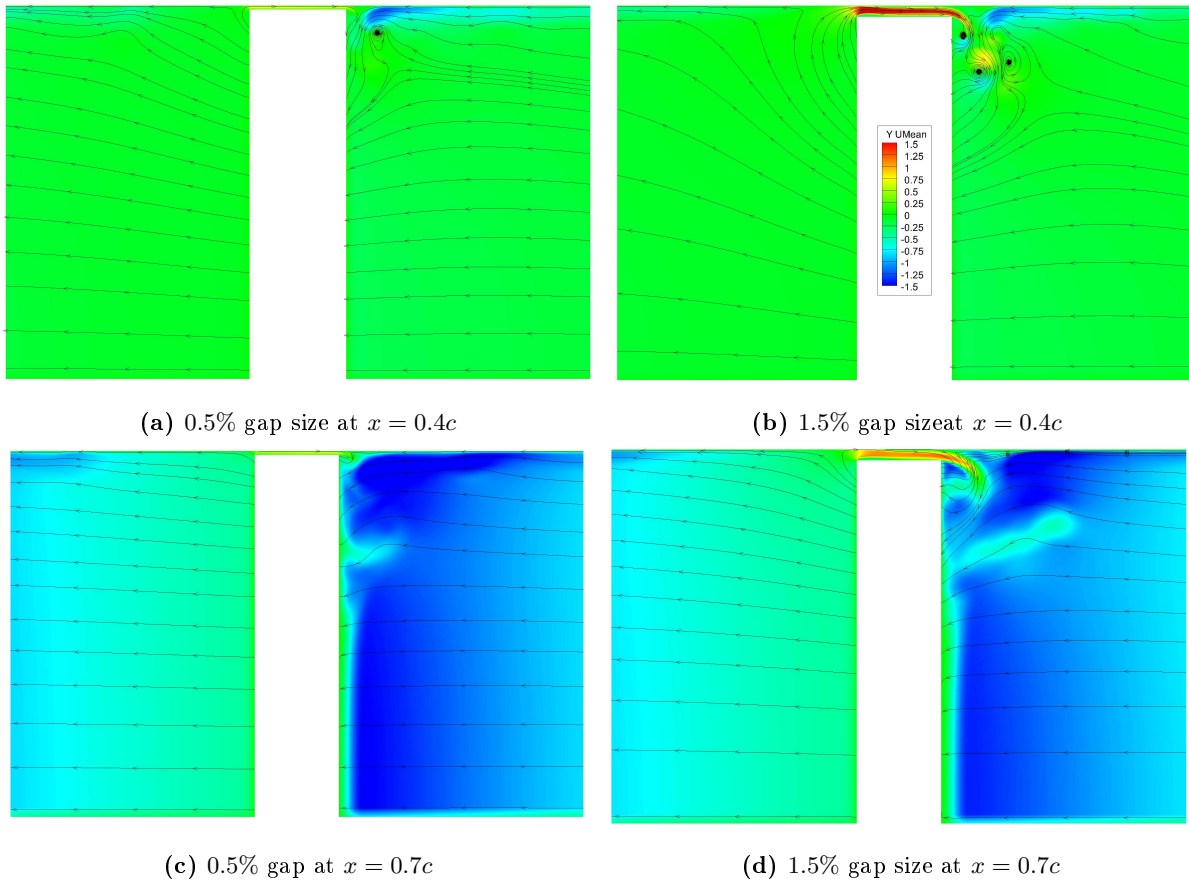


**Figure 6:** The mean  $U_y$  velocity and streamlines at different locations and gap sizes.

Figure 6 presents the detailed view of the flow at two cross-sections at  $x = 0.4C_{ax}$  and  $x = 0.7C_{ax}$  along the blade. The  $U_y$  velocity is shown in this figure along with streamlines. Separation bubble forms a blockage (vena-contracta) effect. As a result, flow that passes above the separation bubble creates a jet flow. The separation bubble begins mixing with the isentropic jet where the separation bubble size (maximum jet contraction) is the maximum as shown in figure 1 [Schabowski and Hodson, 2014]. The jet flow appears only in the high clearance case. This event does not occur in the small clearance case because the separation bubble does not occur for small clearance case. Since the jet flow is stronger in the high clearance case, the effect of this jet extends all the way up to the half-span as shown in figures 4 and 5. The streamlines interact more drastically with the secondary flow in the high clearance case and mix with the main flow as compared to the low clearance case.

The time-averaged mean pressure coefficient distribution along the surface of the blade are evaluated at two span locations for each case. The LES mean pressure coefficients are compared with DNS and experimental data [Koschichow et al., 2014] as shown in figure 7. For each case, there is a favourable pressure gradient along the pressure side of the blade from  $0.1 C_x$  to  $0.6 C_x$ . After this position, flow moves while it is subjected to strong adverse pressure gradient. The tip leakage flow and the main flow interact with each other along the suction side of the blade from  $0.3 C_x$  to  $0.6 C_x$ . Because of this interaction, the mean pressure distribution presents variations around this region. Lowest pressure distribution is observed from  $0.6 C_x$  to the trailing edge along the suction side forward adverse pressure gradient. At the same time, the separation starts from this point ( $0.6 C_x$ ). These situations become more drastic near to the tip region. Furthermore, pressure losses increases drastically near the tip. While pressure increase along the suction side, it decreases along the pressure side due to leakage flow. In the high case, fluctuation of mean pressure coefficient is more because of the tip leakage vortex is drastically interact with other secondary flow structures at near the blade tip.

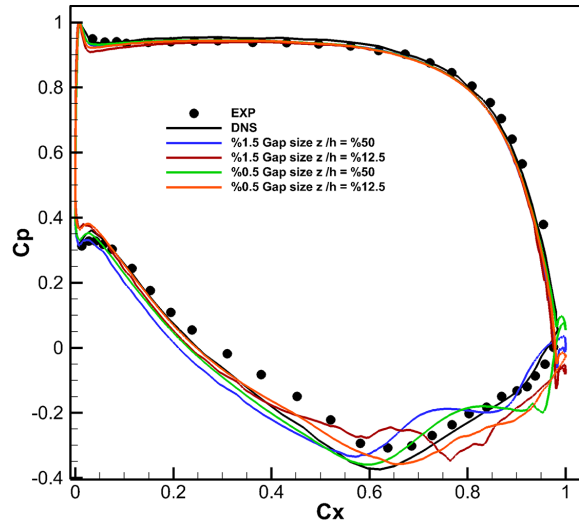


**Figure 7:** The time-averaged mean pressure coefficient distribution along the blade at different span locations.

### Losses

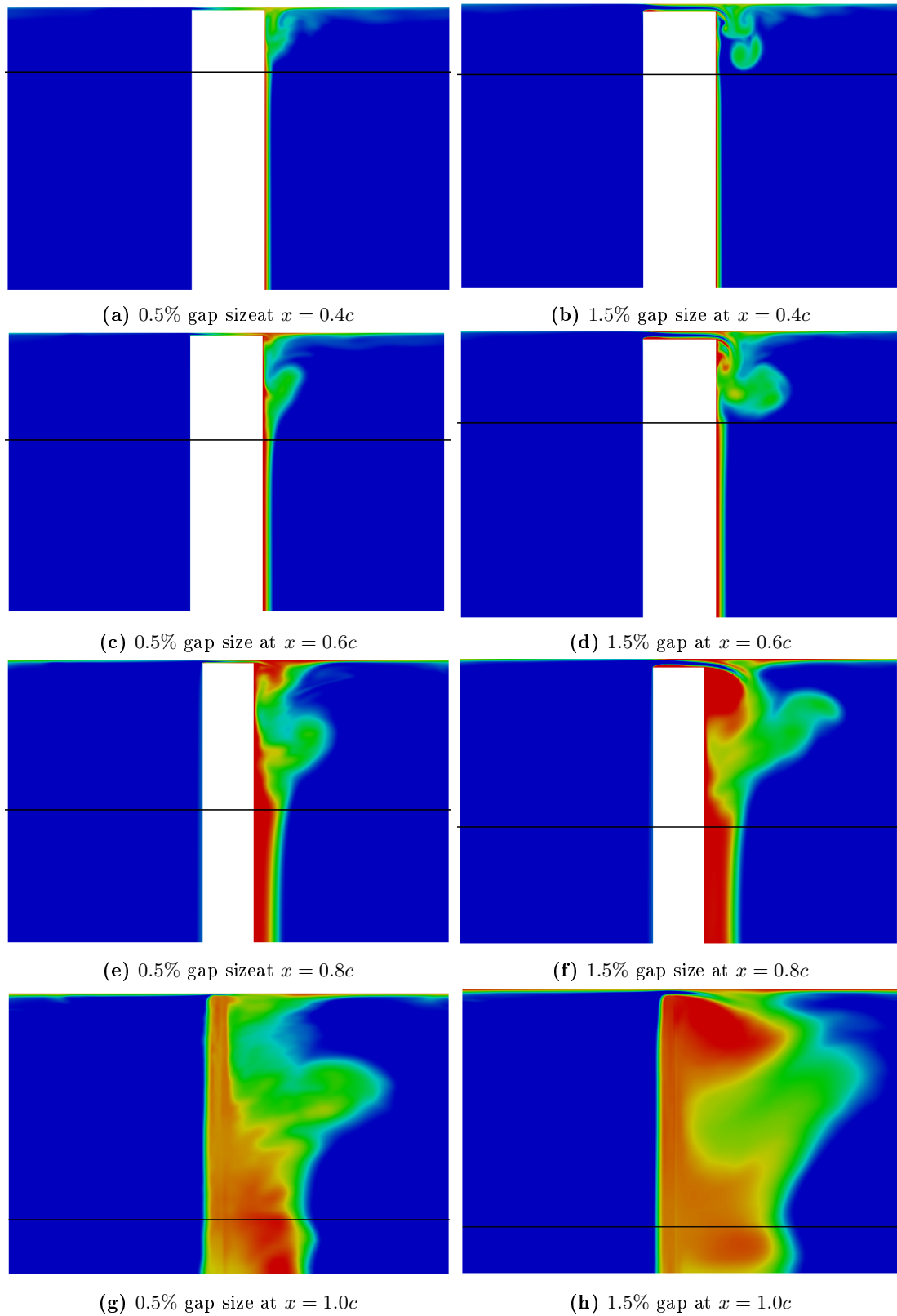
Various loss mechanisms, such as blade boundary layer and trailing edge loss, tip leakage loss, endwall loss, effects of heat transfer and miscellaneous losses occur within the turbine [Lompart et al., 2004]. Only the tip leakage flow losses are examined in this study. The total pressure loss coefficient, which is defined as the relative total pressure at the inlet to the outlet [Lompart et al., 2004] is used in the current study.

$$Y_p = \frac{\bar{p}_{t,in} - p_t}{\bar{p}_{t,in} - \bar{P}_{out}}. \quad (1)$$

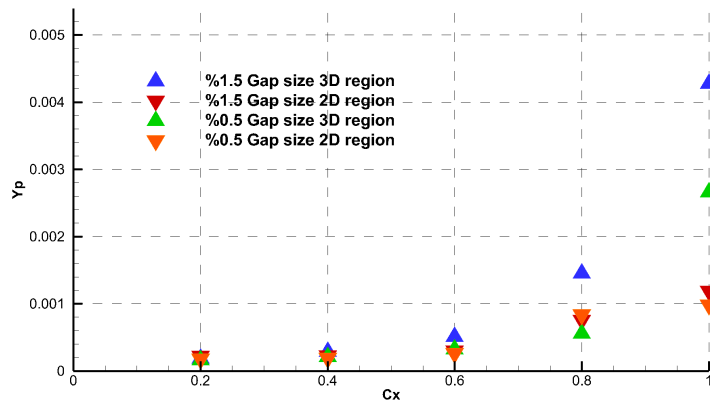
Here,  $\bar{p}_{t,in}$  is the average total pressure of the inlet,  $p_t$  is the local total pressure,  $\bar{P}_{out}$  is the average static pressure of outlet. The total pressure loss coefficient is an important parameter preferred for the numerical model to capture the magnitude and extent of losses caused by the significant flow structures [Basson and Lakshminarayana, 1995]. Furthermore, the accuracy of these losses is influenced by many factors such as turbulence model, governing equation and mesh quality [Basson and Lakshminarayana, 1995]. Total pressure loss due to tip leakage flow is expected to be in the vicinity of the blade tip.

Figure 8 presents a detailed view of the total pressure loss coefficient,  $Y_p$  at four different cross-sections along the blade for small and high clearance cases. As seen in the figure, the losses increase in the flow direction. However, structures that are formed due to tip gap and total pressure loss coefficient show that losses are higher in the high clearance case. In addition, total pressure losses along the chord on the suction side increase from the blade surface to half span in the high clearance case. The major cause of the leakage flow loss is the mixing of the leakage flow and the main flow, while losses within the clearance are relatively low [Zou et al., 2017]. The study of Moore and Adhye (1985) remarked that the increase in total pressure loss coefficient due to flow mixing was almost completely explained by the dissipation of secondary kinetic energy [Cay, 2018]. The maximum total pressure loss is seen at the core of the leakage vortex and the interaction zone of the passage vortex and the leakage vortex in the high clearance case. The increased leakage mass flow rate causes larger and stronger vortices and increases the total pressure loss [Jiang et al., 2015].

In figure 8, the horizontal lines divide planes into two-dimensional (2D) region and three-dimensional (3D) region. The upper side of the black line, which is the three-dimensional region, includes losses due to tip leakage flow, while the bottom of the black line, which is the two-dimensional region, includes losses due to boundary layer separation. Average total pressure losses are obtained in these 2D and 3D regions and presented in figure 9. Losses due to the structures originating from the



**Figure 8:** Total pressure loss coefficient on tangential planes. Contour levels from 0.1 for deepest blue to 1 for brightest red.



**Figure 9:** Average total pressure loss coefficient for 2D and 3D regions at  $x = 0.2C_x$ ,  $x = 0.4C_x$ ,  $x = 0.6C_x$ ,  $x = 0.8C_x$ ,  $x = 1.0C_x$ .

three-dimensional region of high clearance case and both regions of small clearance case are lower than the two-dimensional structures of high clearance case at the leading edge of the blade. Losses of high clearance case in the three-dimensional region are higher than the losses in the two-dimensional region at  $x = 0.6C_x$ . But, losses of 2D and 3D regions are equal to each other in the small clearance case at  $x = 0.6C_x$ . Also, there is not much difference between three-dimensional losses and two-dimensional losses in the small clearance case at  $x = 0.8C_x$ . Losses caused by the tip leakage flow are approximately four times of the losses due to the boundary layer separation at the trailing edge in the high clearance case. Furthermore, the three-dimensional losses are two times higher in the high clearance case than in the small clearance case. The two-dimensional losses are equal in both cases at trailing edge. The separation bubble causes significant total pressure loss in the gap. Losses due to the separation bubble are the highest in the turbine at the high clearance case as shown in figure 10(b). In addition, the separation bubble is mixed with the jet flow and cause loss on the blade tip surface at  $x = 0.8C_x$  in the high clearance case as shown in figure 8. It is not possible to observe these losses in the low clearance case because the separation bubble does not occur. In conclusion, increasing the clearance size causes more losses.

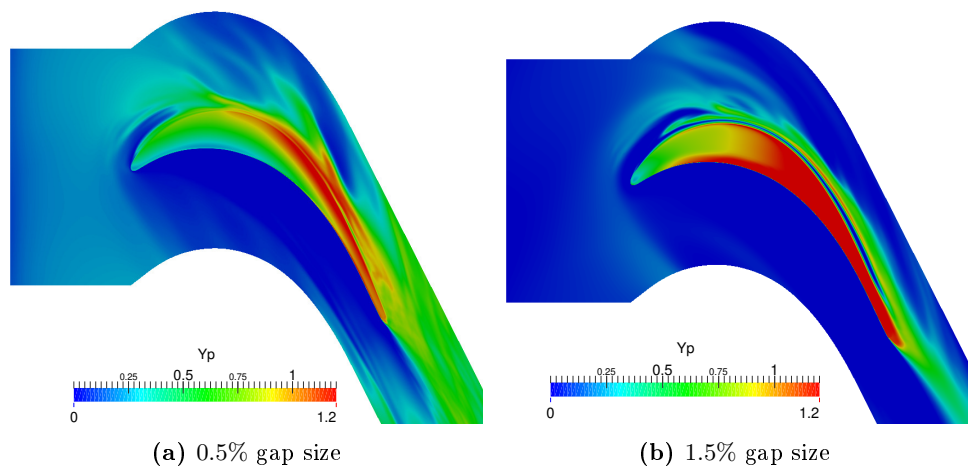


**Figure 10:** Total pressure loss coefficient distribution on the tip of the blade.

## CONCLUSIONS

The main objective of this study is to explore and improve our understanding of the tip leakage flow mechanism and the tip clearance size effect on leakage losses. Two clearance sizes, %0.5 and %1.5 of the span are investigated. Simulations are performed in OpenFOAM using LES solver, pisoFoam. T106 turbine blade profile settled in a linear cascade is utilized for the present study with actual design dimensions. The energy density spectra obtained from a probe data is considered to assess the quality of the LES grid. A decade of  $-5/3$ rd law is observed indicating that the energy carrying structures are resolved in both simulations. Instantaneous flow visualizations indicate that complex secondary flows structures occur as a result of the interaction of the main flow and the leakage flow. Even though that phenomena is seen on both clearance sizes, the effect of leakage flow on the main passage flow increases with an increase of tip clearance size. Such effect extends all the way up to the half-span, indicating the significant alternation of the primary flow on the suction surface due to enhanced leakage for the high clearance case. Besides, leakage flow interaction vortices are bigger in size and carries more energy for 1,5% of clearance case. Such leaking fluid disturbs the main flow on suction side along the axial chord of the blade much more than 0,5% of clearance case. Far from the tip clearance, the time-averaged pressure coefficient distribution agrees well with the DNS data except around the separation region. The leakage flow and the mixing and interaction of the mainstream with the leakage flow result in total pressure loss. The total pressure loss increases in the axial chord direction of the turbine blade. In areas close to the trailing edge of the turbine blade, the total pressure loss extends from blade tip to the half-span. Results demonstrate the need to consider optimum clearance size in turbine blade design.

## References

- Andichamy V. C., Khokhor G. T., Camci C. (2018) *An experimental study of using vortex generators as tip leakage flow interrupters in axial flow turbine stage*, ASME GT2018-76994.
- Basson, A., and Lakshminarayana, B. (1995) *Numerical simulation of tip clearance effects in turbomachinery*, Journal of Turbomachinery, Vol. 117(3) pp. 348-359.
- Cay S.(2018) *Large eddy simulation of secondary flow structures in low-pressure turbine blade*, Master Thesis, Istanbul Technical University.
- Denton J. D. (1993) *Loss mechanisms in turbomachines*, International Gas Turbine and Aeroengine Congress and Exposition ASME 93-GT-435 paper V002T14A001.
- Jiang,D., Luo, H., and Zhang, X. (2015) *Numerical study of the leakage flow on a novel turbine blade tip*, Procedia Engineering, Vol. 99 pp. 413-422.
- Koschichow, D., Froehlich, J., Kirik, I. and Niehuis, R. (2014) *DNS of the flow near the endwall in a linear low pressure turbine cascade with periodically passing wakes*, ASME GT2014-25071.
- Lee, S.W., and Kim, S.U. (2010) *Tip gap height effects on the aerodynamic performance of a cavity squealer tip in a turbine cascade in comparison with plane tip results: Part 1—tip gap flow structure*, Exp Fluids, Vol. 49, pp. 713-723.
- Lei, Q., and Yanpei, Z. (2014) *Turbine blade tip leakage flow control by unsteady periodic wakes of upstream blade row*, JProcedia Engineering, Vol. 80 pp. 202-215.
- Lompart P., Yershov S., Rusanov A. and Szymaniak M.(2004) *Tip leakage main flow interactions in multi-stage hp turbines with short-height blading*, ASME GT2004-53882.
- Morphis G. and Bindon J. P.(1994) *The performance of a low speed one and a half stage axial turbine with varying rotor tip clearance and tip gap geometry*, International Gas Turbine and Aeroengine Congress and Exposition ASME 94-GT-481.

- Tallman , J., and Lakshminarayana, B. (2001) *Numerical Simulation of Tip Leakage Flows in Axial Flow Turbines, With Emphasis on Flow Physics: Part II: Effect of Outer Casing Relative Motion*, of *Turbomachinery*, Vol. 123, pp. 323-333.
- Trehan, R.F., and Roy, B.(1994) *Application of sweep to low pressure turbine cascade blade for tip flow containment*, AIAA:2012-3878.
- Schabowski, Z., and Hodson, H. (2014) *The reduction of over tip leakage loss in unshrouded axial turbines using winglets and squealers*, *Journal of Turbomachinery*, Vol. 136/041001-1.
- Volino R. J.(2017) *Control of tip leakage in a high-pressure turbine cascade using tip blowing*, *Journal of Turbomachinery*. 10.1115/1.4035509, Vol. 139(6), ASME TURBO-16-1176.
- Zou, Z., Shao, F., Li, Y., Zhang, W., and Berglund, A. (2017) *Dominant flow structure in the squealer tip gap and its impact on turbine aerodynamic performance*, *Energy* Vol. 138, pp. 167-184.